Proceedings World Geothermal Congress 2020+1
Reykjavik, Iceland, April - October 2021

Active Basalt Alteration at Supercritical Conditions in IDDP-2 Drill Core, Reykjanes, Iceland

Robert Zierenberg[1], Guðmundur Ó. Friðleifsson[2], Wilfred Elders[3], Peter Schiffman[1], Andrew Fowler[4], Mark Reed[5], David Zakharov[5], and Ilya Bindeman[5]

[1]Dept. Earth and Planetary Sciences, Univ. Calif. Davis, Davis, CA 95616; [2]HS Orka, Svartsengi, 240 Grindavik, Iceland; [3]Universtity of California, Riverside, USA, [4]EHS Support, Portland, Maine; [5]Dept. of Geological Sciences Univ. of Oregon, Eugene OR 974032;

razierenberg@ucdavis.edu

Keywords: Supercritical, mid-ocean ridge, geothermometry, basalt alteration, sheeted dike, high temperature reaction zone.

ABSTRACT

The IDDP-2 drill hole is located in a seawater-recharged, active hydrothermal system on the landward extension of the Reykjanes Ridge. Spot cores recovered from 3648 to 4659 meters depth consist of pervasively altered sheeted dikes. The shallowest cores have an alteration mineral assemblage similar to the producing geothermal reservoir with calcic plagioclase, hornblende, actinolite, epidote, chlorite and quartz. Samples from depths below 3865 m are dominated by intermediate plagioclase and hornblende and do not contain epidote or chlorite. The deepest cored section (4634-4659 m) generally retains a diabasic texture, but all igneous minerals are replaced or have changed composition. Plagioclase retains its igneous texture but now has composition ranging from An_{30} to An_{99}. Igneous augite is replaced by intergrown hornblende, clinopyroxene, and orthopyroxene. Recrystallized magnetite and ilmenite are ubiquitous, along with pyrrhotite. Hydrothermal biotite and olivine (Fo_{58-64}) occur in some samples. Multiple independent mineral geothermometers indicate that peak hydrothermal alteration occurred at ~800°C. Geothermometry on the paragenetically latest alteration suggests that *in situ* temperatures at the bottom of the hole are approximately 600°C. Co-existence of vapor-rich and salt + vapor-rich fluid inclusions suggest that *in situ* conditions are in the brine liquid - vapor field, consistent with the presence of brine in pores indicated by precipitation of halite + K-Fe-Cl salts on the surface of some cores as they dried.

1. INTRODUCTION

The goal of the Iceland Deep Drilling Program (IDDP) is to investigate the feasibility of producing electric power from supercritical geothermal fluids whose chemical properties are shaped by reaction with the host rocks. The IDDP-2 drill hole is of particular interest as it provides the first drill core recovered from the high temperature reaction zone of a seawater-recharged hydrothermal system that is a geochemical analog for black smoker seafloor hydrothermal systems, which are a dominant source of energy and chemical exchange between the lithosphere and the hydrosphere. Details of various aspects of the IDDP-2 project are covered by multiple papers presented at the 2020 World Geothermal Conference. In this paper, we focus on the hydrothermal alteration observed in drill core recovered from seven different depths intervals spanning 3648 to 4659 meters down hole (Friðleifsson et al, 2020 a, b). The bottom part of the hole was angled to intercept the hydrothermal upflow zone that feeds the Reykjanes geothermal field. These cores record the transition from the presently exploited geothermal reservoir at Reykjanes, which extends down to near 3000 m, into the high temperature reaction zone. The deepest cores record evolved seawater water - rock alteration in a sheeted dike complex at temperatures above the supercritical curve at temperatures and well above the brittle-ductile transition for basaltic rock. The observations have important implications for the understanding the processes that control the composition of hydrothermal fluids venting at mid-ocean ridges and challenge the conventional wisdom as to the temperature and mineral assemblages present in the high temperature reaction zones of black smoker systems. We present the results of whole rock and trace element geochemistry (XRF, ICP-MS) from representative samples from each cored interval. Thirty seven polished thin sections were examined using transmitted and reflected light microscopy. Quantitative mineral compositions were determined by electron microprobe.

2. RESULTS AND ANALYSIS

2.1 Lithology and Mineralogy

Details regarding drilling parameters, cored intervals and recovery are provided by Friðleifsson et al., (2020 b) and contained references. Preliminary descriptions of the core are presented in Weisenberger et al. (2017) and Zierenberg et al. (2017). The dominant lithology recovered in all of the cores is fine- to coarse-grained diabasic dikes. With the exception of material from core 8, primary igneous textures are well preserved, but the rocks are pervasively altered and thoroughly recrystallized. Bulk rock major and trace element compositions are comparable to other tholeiitic basalts from the Reykjanes peninsula and fall into the field of trace element enriched (TEE) basalts as defined by Gee et al. (1998). With the exception of elevated loss on ignition (LOI) from hydrous alteration phases, the rocks show little evidence of significant metasomatic additions or subtractions (Fowler and Zierenberg, 2016). The suite of rocks define a weak fractionation trend (Fig. 1). Rocks from core 3 (~3648 m) are the most primitive, with Zr normalized Nb and Y ratios and REE patterns (Fig. 1D) that are slightly displaced towards those of the trace element depleted suite of Gee et al. (1998) (Fowler and Zierenberg, 2016). There is no systematic variation in rock composition with depth. All of the diabases had same primary mineralogy of plagioclase-augite-titanomagnetite with the exception of the uppermost dike (Dike 1) in core 11 (~4635 m) which had sparse (<1%) phenocrysts of olivine. Centimeter scale felsic segregation veins (Felsite on Fig. 1) are present in minor amounts in Core 8 (~4255 m) and deeper samples, and some are invaded by, and not easily distinguished from, more quartz-rich hydrothermal veins. These are discussed in more detail below.

Previous papers discuss the hydrothermal alteration in the main production reservoir, extending down to approximately 3000 m, in the Reykjanes geothermal system (e.g. Lonker et al., 1993; Franzson et al., 2002; Marks et al., 2010; Fowler et al., 2015; Fowler and Zierenberg, 2016). The upper part of the reservoir falls into the Epidote-Actinolite zone of Kristmannsdóttir (1975), but below approximately 2400 m, calcic plagioclase and aluminous hornblende mark the transition into amphibole alteration formed at temperatures above ~320° C (Marks et al., 2010; Fowler et al., 2015; Fowler and Zierenberg, 2016). The IDDP-2 cores are discussed in relation to three alteration zones described below: Hydrothermal Reservoir Transition Zone (Core 3; 3648-3649m), Hornblende-Plagioclase Zone (Cores 5-10; 3865.5-4311.2m), and Pyroxene-Hornblende-Plagioclase Zone (Cores 11-13; 4634.2-4659m). Due to the spot coring and the absence of cuttings (Friðleifsson et al, 2020 b), the boundaries between these zones remain poorly defined.

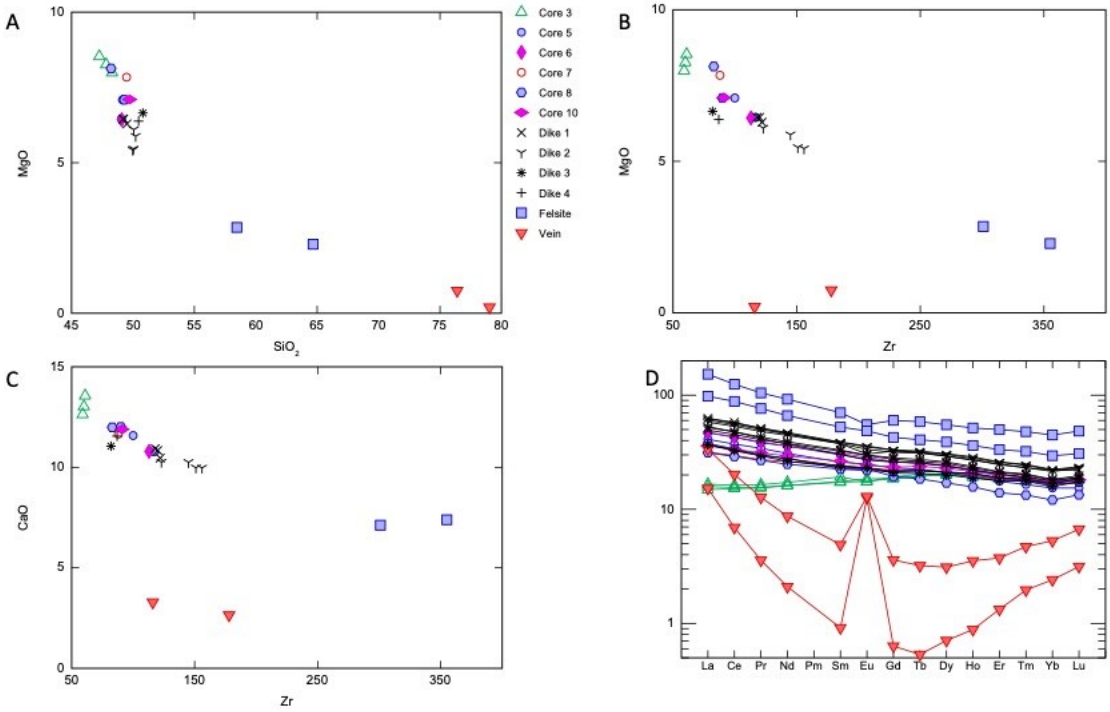

Figure 1: Bulk rock geochemical data. A. MgO versus SiO_2. B. MgO versus Zr. C. CaO versus Zr. D. Chondrite normalized (Sun and McDonough, 1989) rare earth element.

2.1.1 Hydrothermal Reservoir Transition Zone

The rocks recovered in Core 3 contain portions of three dikes separated by two chilled margins. Igneous texture is well preserved. Plagioclase is cloudy but retains its primary crystal outline and zoning. Pyroxene is extensively replaced by amphibole, but pyroxene that has the appearance of primary igneous augite remains. Groundmass and veins are dominated by amphibole, chlorite, epidote quartz and plagioclase. Samples from Core 3 are the only ones that have the same mineral assemblage as the overlying hydrothermal production reservoir: quartz, plagioclase, chlorite, epidote, actinolite, hornblende, diopside, magnetite, ilmenite, titanite, apatite, pyrite, pyrrhotite, isocubanite, chalcopyrite, and sphalerite. The core is extensively veined (Fig. 2A), but in contrast to shallower reservoir rocks, open-space filling veins are absent. The hydrothermal veins are centimeter-scale, discontinuous, anastomosing replacement veins dominated by quartz, plagioclase, amphibole and epidote, many with darker, chlorite-rich selvages. Nearly monomineralic, millimeter-scale veins of amphibole and hydrothermal clinopyroxene that cross-cut the chilled margins change from clinopyroxene in the chilled zone to amphibole in the crystalline portion of the dike. The average composition of the replaced igneous plagioclase in this zone is distinctly more calcic than typical igneous plagioclase or hydrothermal plagioclase in the underling rocks (Fig. 2B). Hydrothermal plagioclase can be distinguished from igneous plagioclase by lower concentrations of Mg and Fe (Marks et al., 2010; Zierenberg et al., 2017) and most of the plagioclase analyzed in Core 3 has relatively low concentrations of Mg and Fe relative to unaltered igneous plagioclase. Hydrothermal clinopyroxene in veins is also calcic and plots along the diopside-hedenbergite join. Interestingly, residual igneous clinopyroxene is also more calcic (Fig. 2C) than typical igneous augite and tends to have lower concentrations of trace elements, including Na and Ti compared to augite in least altered diabase. Core 3 diabases are the least fractionated and most calcic rocks recovered (Fig. 1C), but the microprobe data suggest that the calcic nature of both plagioclase and pyroxene is due to hydrothermal exchange. Amphibole compositions show a range from actinolite to aluminous hornblende (Fig. 2D). The presence of calcic plagioclase and aluminous hornblende replacing igneous and vein minerals indicate that this rock is not in textural or mineralogical equilibrium, but instead is undergoing prograde replacement of epidote-actinolite alteration by minerals indicative of amphibole facies alteration.

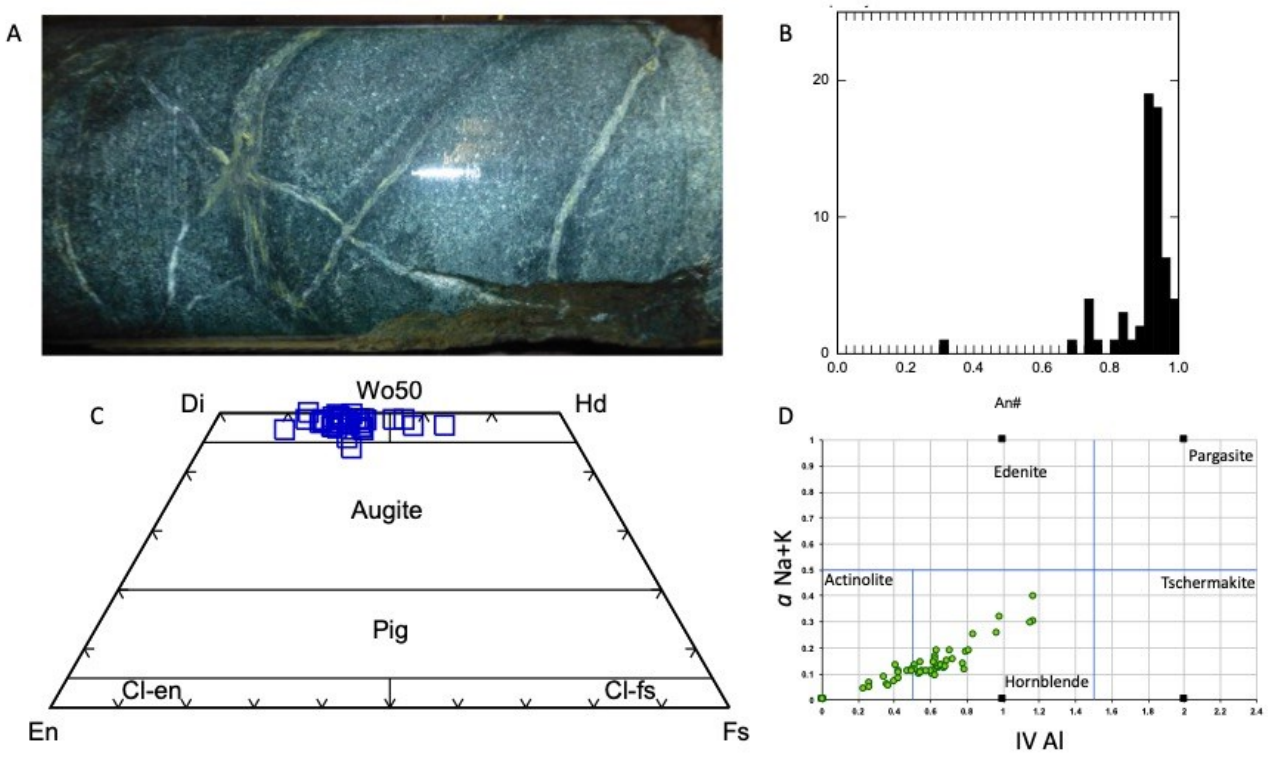

Figure 2: A. Diabase dike (Core 3, 3648.5 m), with multiple generations of Qtz-Plag-Epidote-Amphibole replacement veins. B. Anorthite content of groundmass plagioclase. C. Pyroxene composition including remnants of igneous pyroxene and hydrothermal veins. D. Activity of Na+K versus tetrahedral aluminum of amphiboles, which vary from actinolite to hornblende.

2.1.2 Hornblende-Plagioclase Zone

Cores 5-10 (3865 to 4311m) are grouped based on the similarity of the alteration observed in this interval. In general, each core recovered a portion of a single dike interior ranging from fine-grained to medium-grained diabase. One exception is Core 8, which contains fine-grained diabase from the quenched margin of a dike. The limited core recovered from Core 8 are the most intensively deformed and veined samples recovered, with multiple stages of 1-3 mm quartz-plagioclase-amphibole ± trace biotite veins. The first occurrence of a centimeter scale 'felsic segregation vein' is found at 4309.97 m in Core 10, a 1-2 cm wide vein of plagiogranite that cross cuts the diabase with no chilled contacts and rather diffuse boarders. An adjacent sample from 9 cm deeper (4310.06 m) marks the first occurrence of biotite as an alteration mineral in the matrix of the rock.

With the exception of Core 8, samples from the Plag-Hornblende zone are notable for their lack of deformation and veining. Rather inconspicuous, monomineralic hornblende veins ~1 mm wide are the most common (Fig. 3A) with an abundance of 1-3 per meter of core recovered. Although igneous textures are well preserved, the rocks are pervasively altered with few to no original mineral compositions preserved. Plagioclase crystals have igneous morphology and twinning, but have a dusty appearance owing to abundant microscale fluid inclusions and iron oxide, as well as ubiquitous very fine-grained apatite needles. Plagioclase shows a wide range of compositions (Fig. 3B) and generally has low concentrations of Mg and K compared to primary igneous crystals. Igneous augite is nearly completely replaced, and much is pseudomorphed by hornblende with patches of residual augite (Fig. 3C). Amphibole compositions generally plot in the hornblende field, with less abundant edenite (Fig. 3D). Trace amounts of cummingtonite are present in samples from cores 7 and 8. Igneous titanomagnetite shows extensive oxidative exsolution to magnetite-ilmenite. Pyrrhotite (± copper-iron sulfide) is a common accessory mineral present in low abundance (<1%). The presence of calcic plagioclase and aluminous hornblende, and the lack of albite, epidote, and chlorite, define the Plagioclase – Hornblende alteration zone, which formed at temperatures equivalent to amphibolite metamorphism (>450°C), albeit at lower pressures.

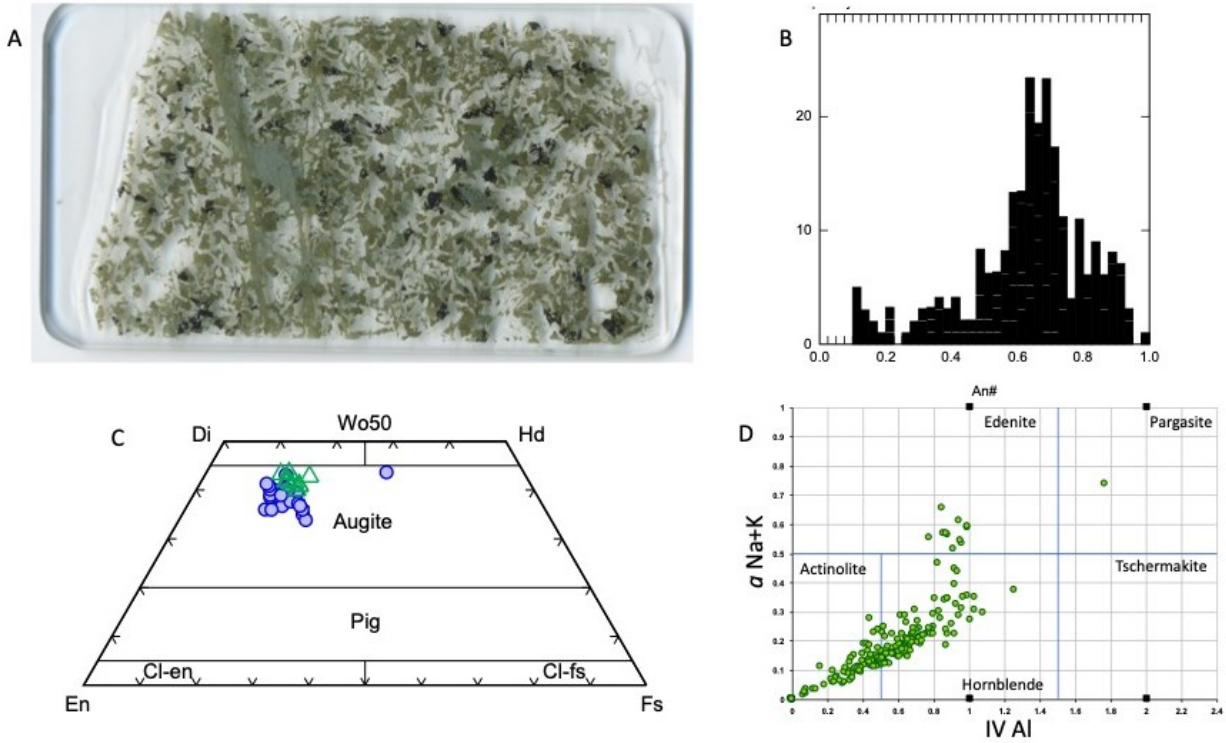

Figure 3: A. Thin section scan of altered diabase dike (Core 6, 3869.85 m) cross cut by green amphibole vein. B. Anorthite content of groundmass plagioclase. C. Pyroxene composition including remnants of igneous pyroxene and hydrothermal veins (blue dots). Green triangles are igneous augites from a relatively unaltered dike. D. Activity of Na+K versus tetrahedral aluminum of amphiboles, which generally vary from actinolite to hornblende, with some plotting in the edenite field.

2.1.3 Pyroxene-Hornblende-Plagioclase Zone

Cores 11-13 (4634-4657 m) were recovered from the bottom of the hole and contain a near continuous record of the deep alteration in the hydrothermal upflow zone that feeds the Reykjanes geothermal system (Friðleifsson et al., 2018). Portions of four diabase dikes were recovered separated by three chilled margins. In each case, the shallower dike was chilled against (was younger than) the underlying dike. No evidence of contact metamorphism of the older dikes was observed in thin sections that preserve the dike margins. The dikes are numbered 1-4 from shallowest (youngest) to deepest (oldest). All have similar compositions (Fig. 1) and textures with the exception of Dike 1 which contains sparse (<1%) phenocrysts of olivine. The original mineralogy of the dikes was plagioclase-augite-titanomagnetite. One thin section from Dike 2 (4650.67 m) contains a single 7 mm xenocryst of orthopyroxene, which is the only observed igneous orthopyroxene in any of the samples. A nearby sample (4649.73 m) has xenocrysts of plagioclase up to 5 mm long.

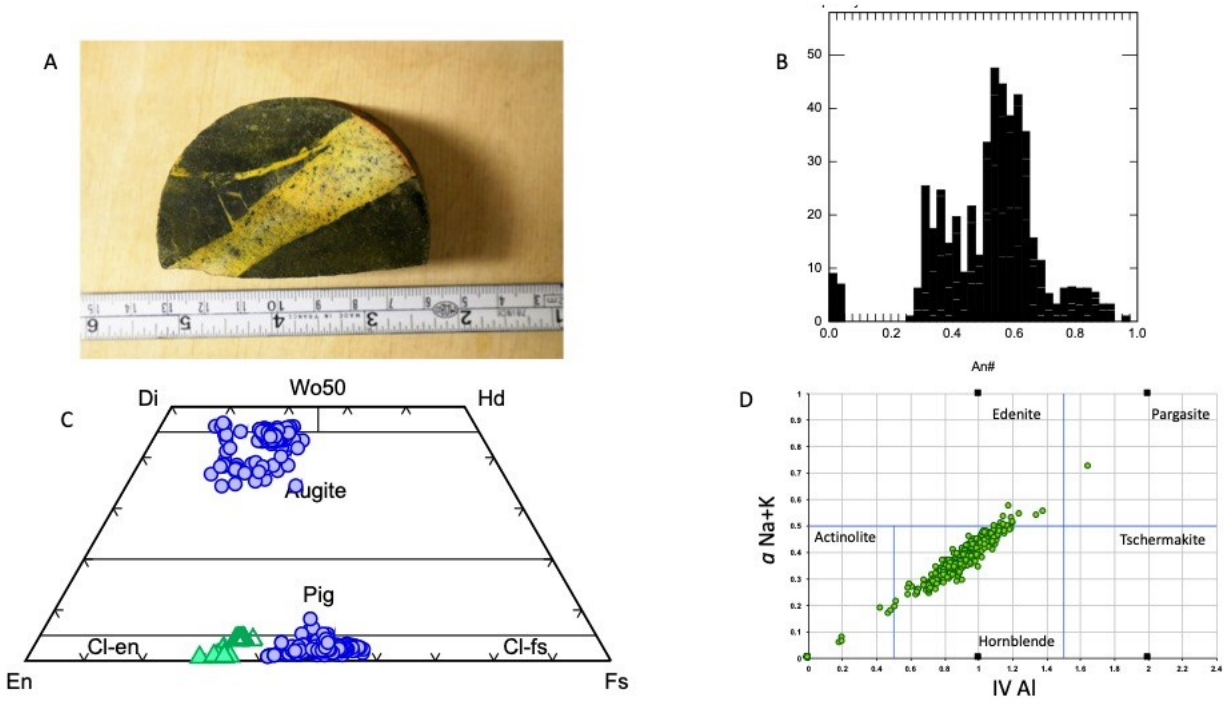

Figure 4 A. Diabase dike (Core 11, 4635.11 m) cut by qtz-plag-biot vein. The yellow stain is from K-Fe-Cl salts precipitated from pore fluid after the core was cut. B. Anorthite content of groundmass plagioclase. C. Hydrothermal pyroxene compositions (blue circles). Orthopyroxene replacing olivine (open triangles) and an opx xenocryst (filed triangles) are more magnesium rich. D. Activity of Na+K verses tetrahedral aluminum of amphiboles.

Igneous texture is relatively well preserved, but minerals do not preserve their original compositions and the rocks are pervasively altered. Plagioclase- and quartz-rich veins (Fig. 4A) and segregations are more common compared to the intervals cored above, but still make up only a minor (<1%) component of the rock. The felsic dikeletts and veins cut the diabase at various angles relative to the core axis and range from a few mm to 3 cm thick. Most of the felsic veins have distinct, but somewhat diffuse, borders and, in some cases, crystals of plagioclase can be traced from the diabase wall rock into the vein interior. In these cases, the plagioclase in the diabase is cloudy and filled with inclusions, whereas the portions of the plagioclase crystal in the vein are clear, similar to other plagioclase in the vein interior.

The distinction between igneous differentiates that fall on the fractionation trend of the diabase dikes (Felsite, Fig. 1) and more quartz-rich veins with a significant hydrothermal component (Vein, Fig. 1D) is not always readily apparent in hand specimens. Most felsic veins have sparse inclusions of partially digested hydrothermally altered wall rock. Euhedral biotite, interpreted to be phenocrysts, occurs in some of the veins. The biotite phenocrysts in the veins generally has higher Fe, Cl and F concentrations than does hydrothermal biotite in the altered diabase matrix. At least one quartz-rich felsic vein is bordered by altered diabase with finer-grained texture suggesting the diabase was partially quenched by emplacement of the felsitic material, but most lack any distinguishable selvages. The veins seem to range from normal igneous segregations of dacitic composition (Felsite, Fig. 1) to those with a significant hydrothermal component that partially replace the rock fabric (Vein, Fig. 1). The felsite dikeletts have elevated REE concentrations with chondrite normalized patters that match the diabases (Fig. 1D), as would be expected if they were the last residue of fractional crystallization. In contrast, the veins have distinctly lower REE concentrations with strong enrichment of the light REE, weaker enrichment of heavy REE and distinctive positive Europium anomalies (Fig. 1D). This REE pattern matches those from hydrothermal fluid at Reykjanes and mid-ocean ridge vent fluids (Fowler et al., 2019), as well as those in hydrothermal epidote in veins cross cutting core samples recovered from the Reykjanes production reservoir (Fowler and Zierenberg, 2015).

Only one significant mineralized, open-fracture vein was recovered during the coring at a depth of 4637.80 m. The fracture forms one border of a 2 cm quartz-plagioclase-potassium feldspar vein with minor biotite, the only observed occurrence of K-feldspar in the core. The fracture surface is coated with euhedral crystals of biotite that is overgrown by doubly terminated euhedral quartz crystals (Zierenberg et al., 2017; Friðleifsson et al, 2018, Bali et al., 2020). This is the latest paragenetic stage of mineralization observed in the recovered core and is discussed in more detail below.

Plagioclase alteration is similar to the overlying Amphibole-Plagioclase alteration zone. Plagioclase retains its original igneous morphology, but the crystals are cloudy due to abundant fluid/vapor and iron oxide inclusions. Hydrothermal plagioclase replacing igneous plagioclase has a narrower range of compositions compared to the overlying Amphibole Zone, and the peak of the histogram is at slightly lower anorthite (An) number (Fig 4B). Potassium contents of plagioclase from the pyroxene zone increase with decreasing An number, and although they are low (mole fraction <0.04), they are distinctly elevated relative to rocks at shallower depths. The defining feature of the pyroxene-hornblende-plagioclase zone is the occurrence of hydrothermal clinopyroxene and orthopyroxene accompanying amphibole in replaced igneous augite. Clinopyroxene, orthopyroxene and amphibole are intergrown at all spatial scales (Fig. 5), including grains too small to be analyzed with a 10 µm electron beam. The compositional range of hydrothermal clinopyroxene overlaps that of igneous augite but extends to less calcic and more magnesium

rich compositions (Fig. 4C). The hydrothermal clinopyroxene also has lower concentrations of minor elements, such as Al and Ti. No igneous augite could be identified in the rocks form this zone. Hydrothermal orthopyroxene is mostly more iron rich than clinopyroxene (Fig. 4C). A large orthopyroxene xenocryst was analyzed from Dike 2 (4650.67 m). It is distinguishable from the hydrothermal opx by having higher concentrations of Mg and lower concentrations of Mn. Orthopyroxene is also present in Dike 1 where it forms a replacement halo around rare olivine phenocrysts due to interaction with silica-rich hydrothermal fluids. These orthopyroxenes are even more enriched in Mg compared with the xenocryst and they have lower Ca. The residual olivine is significantly more Fe-rich (Mg# 58-64) than olivine in equilibrium with tholeiitic basalt (Mg# 80-90). One sample from near the bottom of the hole (4654.15m) contains zones of granoblastic clinopyroxene with minor opx, amphibole, and calcic plagioclase. (Fig. 5C). Amphibole is the dominant mafic mineral in this zone and most of the analysis are consistent with hornblende (Fig. 4D), with a single occurrence of cummingtonite at (4635.11 m). Magnetite and ilmenite are ubiquitous. In contrast to zones above where mt-ilm preserve relict igneous texture with common oxidative exsolution textures (Fig. 6A), both minerals occur as rounded to subhedral crystals typical of metamorphic textures (Fig 6B). Biotite (Fig. 5D) occurs as a dispersed alteration phase throughout Dikes 1and 2 and the uppermost part of Dike 3, but is not observed below ~4651.5 m. Apatite is a ubiquitous accessory phase and most samples contain pyrrhotite, with less abundant Cu-Fe sulfide.

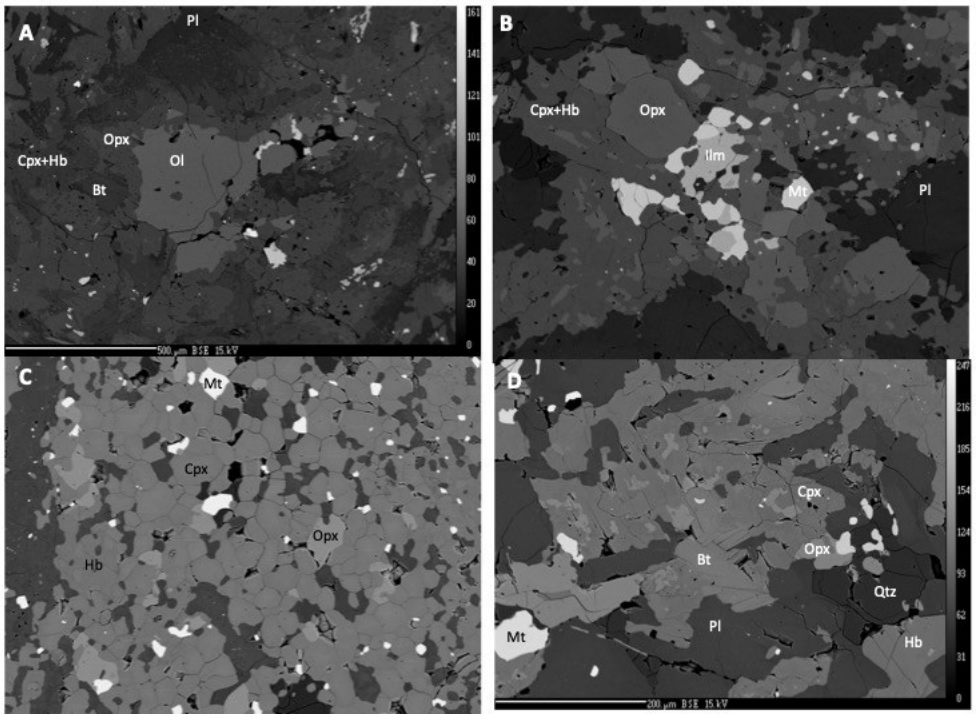

Figure 5 A. Back scattered electron images (BSE) A. Residual olivine (Ol), overgrown by orthopyroxene (Opx). The main alteration is to plagioclase (Pl), clinopyroxene (Cpx) and hornblende (Hb), which are not easily distinguishable in the BSE images, orthopyroxene and biotite (Bt) (Core 11, 4634.48 m). B. Intergrown orthopyroxene, clinopyroxene, hornblende, plagioclase, magnetite (Mt), and ilmenite (Ilm) (Core 12, 4651.64 m). C. Granoblastic clinopyroxene intergrown with orthopyroxene and minor hornblende with interstitial plagioclase (Core 13, 4654.16 m). D. Intergrown orthopyroxene, clinopyroxene, hornblende, biotite, plagioclase, and quartz (Qtz) (Core 12, 4649.24 m).

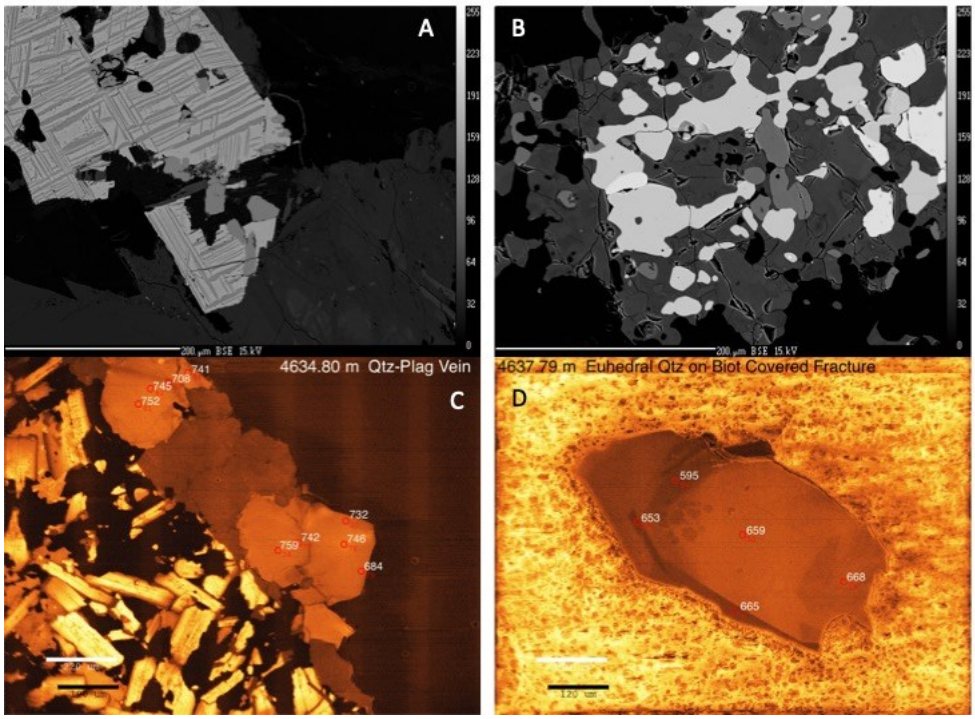

Figure 6. Back scattered electron (BSE) and cathode luminescence (CL) images. A. Igneous magnetite (lightest) intergrown with ilmenite oxidative exsolution lamella. (Core 8, 4254 m). B. Metamorphically recrystallized magnetite (brightest) and ilmenite (next brightest with orthopyroxene (light grey), clinopyroxene, hornblende, and plagioclase (darkest). (Core 13, 4653.25 m). C. CL image of early, high temperature quartz (bright orange) – plagioclase (brown) vein on the edge of a diabase fragment (yellow plagioclase, non-luminescent hornblende). Red numbers and circles designate probe spots, the white numbers are temperatures (°C) calculated from the titanium content. D. CL image of euhedral quartz crystal deposited on biotite overgrowing a late-stage open fracture. Higher titanium (higher temperature) results in brighter luminescence and highlights growth zoning in the quartz (yellow is epoxy grain mount).

3. TEMPERATURES OF ALTERATION

3.1 Peak Alteration Temperatures

Several mineral geothermometers were employed to document the temperature history of the alteration minerals. Detailed presentation of the geothermometry data is beyond the scope of this paper, so only general summaries of the data are presented to 1) address peak alteration temperatures for each of the geothermometers, and 2) constrain the present day temperature of the active geothermal system using geothermometry data from the latest paragenetic stages.

The clinopyroxene-orthopyroxene geothermometer of Anderson et al. (1993) was employed to constrain early, high temperature hydrothermal alteration. Touching pairs of pyroxenes were analyzed. Temperatures range from near magmatic values down to ~700° C and average 825°C ±65 (n-236) (Fig. 7A). These temperatures provide evidence for fluid rock interaction well above the commonly assumed brittle ductile transition in basalts (~600°C). Pyroxene is intimately intergrown with amphibole, the highest temperature hydrous alteration phase. Touching plagioclase-hornblende pairs show a narrow range of temperatures, calculated using the Hora et al. (2013) spreadsheet to implement the Holland and Blundy (1994) geothermometer. The mean temperature (785°C ±39, n=276; Fig. 7B) is below that calculated using the pyroxene geothermometer, owing to the skewed distribution of higher temperatures preserved by the pyroxenes. The peak of the histograms for both geothermometers largely overlap at approximately 800°C, as would be expected for alteration that shares the earliest paragenetic stage, and this temperature is interpreted as peak hydrothermal alteration.

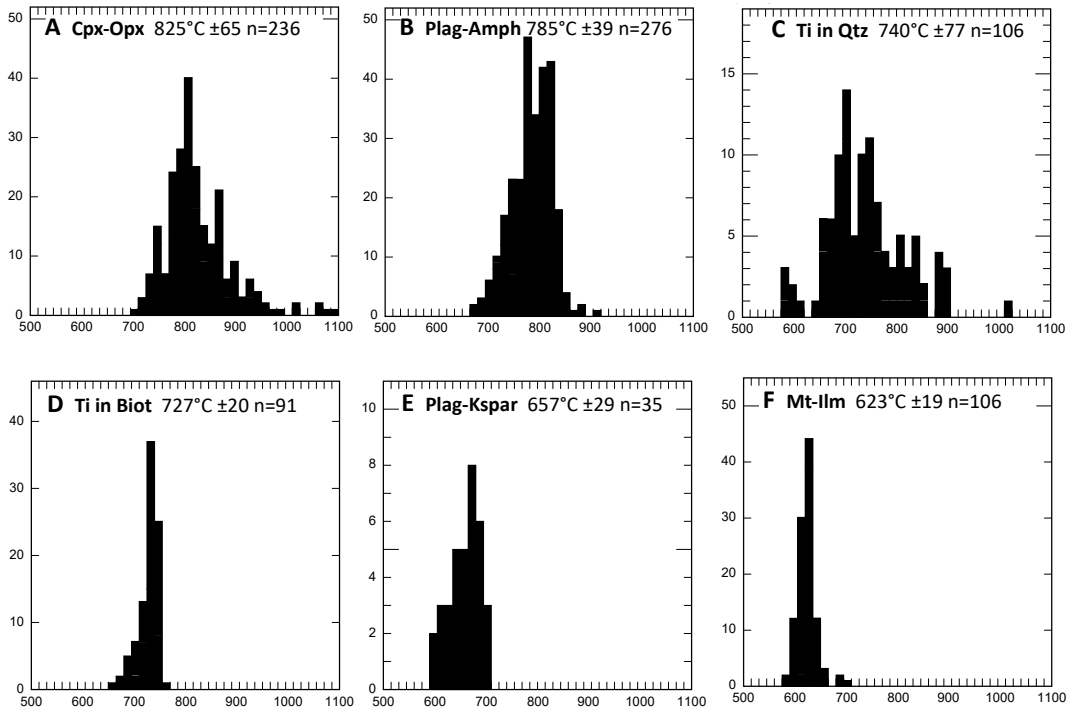

Figure 7. Temperature histograms showing mean temperature ± 1 standard deviation, n = number of analyses. A. Clinopyroxene-Orthopyroxene. B. Plagioclase-Hornblende. C. Titanium in Quartz. D. Titanium in Biotite. E. Plagioclase-K-feldspar. F. Magnetite-Ilmenite.

Titanium in quartz temperatures were calculated using the calibration of Huang and Audetat (2012) assuming a pressure 450 bas (cold hydrostatic recharge) and corrected assuming a TiO_2 activity of 0.53 to reflect equilibrium with ilmenite as the saturated Ti phase, following the approach of Reid et al. (2011). The large range of calculated temperatures is a reflection of the broad paragentic stages of quartz deposition. Quartz occurs primarily in the felsic segregations and veins, which span the paragenetic history from earliest plagiogranite 'dikelets', symplectic intergrowths of quartz-plagioclase, high temperature quartz-plagioclase (± biotite) veins (Fig. 6C), late stage quartz-plagioclase-K-feldspar veins, and latest euhedral quartz overgrowing hydrothermal biotite coating an open fracture (Fig. 6D). The latest stage quartz is used to constrain maximum present-day *in situ* temperatures, as discussed below. The titanium content of biotite can also be used as a geothermometer (Henry et al., 2005). Biotite occurs in some quartz-plagioclase segregation and veins and is intergrown with the other alteration phases in Dikes 1, 2 and the uppermost part of Dike 3. Some sections of the core in the interval where biotite is present are coated with a yellow salt that formed on the surfaces of cut core as pore fluid evaporated when the core dried (Zierenberg et al., 2017). Analysis of this salt by energy dispersive spectrometry in the electron microprobe showed that it is predominantly K-Fe-Cl, and some is accompanied by Cu, Zn, and Mn and halite. Two distinct K-Fe-Cl minerals have subsequently been described as daughter minerals in fluid inclusions in quartz from these depths Bali et al. (2020). Biotite is not expected to form as an alteration mineral in low-K midocean ridge tholeiitic basaltic dikes. The restriction of biotite alteration to the interval around late stage veins with K-feldspar and biotite is consistent with reaction of the basaltic dikes with a high salinity K-Fe-Cl rich brine formed by condensation from supercritical seawater. The narrow temperature peak at ~725°C (Fig. 7D), calculated using the Ti in biotite geothermometer (Henry et al., 2005), is consistent with a sudden, localized appearance of K-rich brine following peak alteration that formed the dominant Plagioclase-Amphibole-Clinopyroxene-Orthopyroxene alteration. A pressure drop related to a fracturing event could cause supercritical seawater to phase separate by condensation of a high salinity brine. Potassium feldspar only occurs in one Quartz-Plagioclase-K-feldspar vein at 4637.79 m. The plagioclase-K-feldspar geothermometer (Putirka, 2008) gives an average temperature of 657°C (Fig. 7E), with a relatively narrow range of temperatures, consistent with a single paragenetic event. The lowest temperature recorded in this vein is ~600°C.

The magnetite-ilmenite geothermometer (Anderson et al. 1993; Ghiorso and Evans, 2008) was attempted on samples from Core 8 (4254 m) to near the bottom of the hole (4656 m). Magnetite-ilmenite in contact in oxidative exsolution intergrowths (Fig. 6A) in titanomagnetite from Cores 8 and 10 do not plot on the Mg-Mn equilibrium line of Bacon and Hirschmann (1988), and do not produce usable temperature information. In contrast, intergrown Mt-Ilm grains in the Cores 11-13 have grain shapes and grain boundaries indicative of metamorphic equilibrium (Fig. 6B), and pass the Bacon and Hirschmann (1988) criteria for chemical equilibrium. The Mt-Ilm temperature histogram shows a narrow range (Fig. 7F) with minimum temperatures again of 590-600°C. While the biotite and two feldspar temperature ranges are consistent with deposition of these minerals over a restricted temperature interval related to their paragenetic stage, Mt-Ilm were present throughout the extended alteration history. Mt-Ilm typically give lower temperatures relative to silicate geothermometers (e.g. Schiffman et al. 2012) due to the lower closure temperature for the oxides. Our interpretation of the Mt-Ilm temperatures is that they are continuing to exchange Fe-Ti during hydrothermal alteration and cooling, and as such they are more representative of *in situ* temperatures as opposed to peak alteration temperatures.

3.2 Present Day Temperature

Minimum temperatures for Ti-quartz, plagioclase-K-feldspar and magnetite-ilmenite are all in the 590-600° C range. In order to try to constrain the maximum present-day temperatures, we focused on the latest, cross cutting paragenetic event, which is the biotite-

quartz coated open fracture that formed on the edge of a quartz-plagioclase-K-feldspar vein at 4637.79 m. Cathode luminescence was used to evaluate the growth history of the quartz in these veins (Fig. 6C, D). The latest stage of quartz growth gives the lowest temperature (590-600°C). The convergence of three independent mineral geothermometers at ~600°C is permissive evidence for the present-day temperature at the bottom of the drill hole. Hand-picked separates of hydrothermal biotite and doubly terminated euhedral quartz were run for oxygen isotope analysis. Because the quartz crystals nucleated on and overgrow the biotite, they did not form at the same time, and therefore may not meet the strict requirement for equilibrium growth. None-the-less, they likely formed in close succession from the same or similar, fluids. The oxygen isotope value obtained on the biotite separate was 3.18‰ (relative to VSMOW); two analyses of quartz gave 6.67‰ and 6.58‰. If we assume isotopic equilibrium, we calculate a temperature of 640°C ±10° using the fractionation equation in Zheng (1993), which falls between the Ti in biotite and Ti in quartz temperatures for these samples. The isotopic value of the water from which these minerals precipitated would be ~4.6‰, consistent with extensive exchange of seawater with basalt at elevated temperature at low water to rock ratio.

Based on the convergence of multiple geothermometers, we propose that the present day *in situ* temperature at the bottom of the hole is approximately 600°C. While the mineral geothermometers only constrain the maximum temperature at the time of drilling, the presence of olivine and orthopyroxene and the absence of hydrous alteration phases, such as serpentine and brucite, argues that present day temperatures must be greater than ~550°C. Temperature estimates based on mineral geothermometers have subsequently been confirmed by analyses of fluid inclusions in quartz from the same samples reported on above. Fluid inclusions are either vapor dominant or salt +vapor dominant, consistent with phase separation of seawater at temperatures above the critical curve. Bali et al. (2020) report homogenization temperatures of 600°C ±20°, and salt rich inclusions contain halite and two yellow K-Fe-Cl minerals along with Cu-Fe sulfide. A pressure temperature log was run in IDDP-2 just prior to coring at the bottom of the hole (Friðleifsson et al, 2018), which confirmed the presence of hydrothermal feed zones below 4500 m. The measured temperature of 426°C at 340 bars falls exactly on the two phase curve for seawater salinity (Driesner and Heinrich, 2007), consistent with active phase separation of a supercritical fluid of seawater origin at the pressures imposed by the hydrostatic head in the drill hole at the time of the measurement.

4. CONCLUSIONS

The Iceland Deep Drilling Project has succeeded, for the first time, in recovering core samples of sheeted dikes altered at supercritical temperatures in an hydrothermally active, seawater-recharged convective geothermal system that is analogous to those that form black smokers on mid-ocean ridge spreading centers. Sheeted dikes that retain their igneous textures are pervasively altered, but little metasomatized. No minerals with primary igneous compositions are retained. At depths below 4500m the alteration mineral assemblage is calcic plagioclase, hornblende, clinopyroxene, orthopyroxene, ±olivine, magnetite, ilmenite, apatite, pyrrhotite, ±Cu-Fe sulfide, ±quartz. Peak hydrothermal alteration occured at approximately 800°C due to interaction of crystalline diabase with single phase supercritical seawater. Paragenetic relationships, including cross cutting replacement veins, record progressive alteration and cooling. As the system cooled to approximately 725°C some of the rocks reacted with a high-salinity, K-Fe-Cl rich fluid forming hydrothermal biotite, and in one vein, K-feldspar. The appearance of a brine is consistent with supercritical phase separation of seawater by brine condensation (as opposed to vapor formation by boiling), plausibly due to sudden pressure release during fracturing. K-Fe-Cl salts were locally trapped in the rock pore space and are present in fluid inclusions in quartz. The system has continued to cool and multiple geothermometers record late-stage alteration at temperatures as low as 590°C, which provides an upper limit on the temperature of the rock at the time of coring. The presence of unaltered olivine and orthopyroxene in an active geothermal system requires temperatures to be above the upper stability limit of serpentine, approximately 550°C. Supercritical seawater entering the bore hole below 4500 m during pressure-temperature logging phase separated at the pressure imposed by the fluid head in the bore hole (340 bars) and was therefore constrained by the invariant curve to the measured temperature of 426°C. Prevailing wisdom among the seafloor hydrothermal community would suggest that fluid rock interaction at temperatures above the brittle ductile transition in basalts (~600°C) is limited and that seawater/rock reactions that control seafloor hydrothermal vent fluid composition include minerals such as intermediate plagioclase, quartz, epidote and actinolite. Results from the IDDP-2 drilling require a re-evaluation of the mineralogy and temperature of the high temperature reaction zones that underlie black smoker systems.

ACKNOWLEDGEMENTS

The IDDP-2 drilling was funded by HS Orka, Statoil (Equinor), Landsvirkjun, Orkuveita Reykjavíkur, and the National Energy Authority in Iceland. The IDDP-2 well has also received funding from the European Union's HORIZON 2020 research and innovation program under grant agreement No 690771 to DEEPEGS. Funding for obtaining spot cores at Reykjanes and elsewhere was provided by ICDP and the US NSF (grant no. 05076725). All these are greatly acknowledged.

REFERENCES

Andersen, D.J., Lindsley, D.H., and Davidson, P.M., 1993, QUILF: A PASCAL program to assess equilibria among Fe-Mg-Mn-Ti oxides, pyroxenes, Olivine, and quartz. Computers &Geosciences. 19: 1333-1350.

Bacon, C.R. and Hirschmann, M.M., 1988, Mg/Mn partitioning as a test for equilibrium between coexisting Fe-Ti oxides. American Mineralogist. 7:57-61.

Bali, E., L.E. Aradi, A. Szabo, R.A. Zierenberg, G.Ó. Friðleifsson, C. Szabo. Fluid inclusions in the deepest part of the IDDP-2 drill core, Reykjanes Peninsula, Iceland. Proceedings World Geothermal Congress, (2020).

Driesner, T. and Heinrich, C.A., 2007, The system H2O-NaCl. Part I. Correlation formulae for phase relations in temperature-pressure-compostion space from 0 to 1000° C, 0 to 5000 bar, and 0 to 1 XNaCl. Geochem. Cosmochim. Acta, 71:4880-4901.

Fowler, A.P.G. and Zierenberg, R.A., 2015, Rare Earth Element Concentrations in Geothermal Fluids and Epidote from the Reykjanes Geothermal System, Iceland. Proceedings World Geothermal Congress 2015, Melbourne Australia, 19-25 April, 2015, 10p.

Fowler, A.P.G., Zierenberg, R.A., Schiffman, P., Marks, N. and Friðleifsson, G. Ó., 2015, Evolution of fluid-rock interaction in the Reykjanes geothermal system, Iceland: Evidence from Iceland Deep Drilling Project core RN-17B. Journal of Volcanology and Geothermal Research. 302:47-63.

Fowler, A.P.G. and Zierenberg, R.A., 2016, Elemental changes and alteration recorded by basaltic drill core samples recovered from in situ temperatures up to 345° C in the active, seawater-recharged Reykjanes Geothermal System, Iceland, Geochem. Geophys. Geosyst., 17, doi:10.1002/2016GC006595.

Fowler, A.P.G. Zierenberg, R.A., Reed, M., and Palandri, J., Óskarsson, F., and Gunnarson, I., 2019, Rare earth element systematics in boiled fluids from basalt-hosted geothermal systems, Geochimica et Cosmochimica Acta, v. 244, p. 129-154.

Franzson, H., Thordarson, S., Bjornsson, G., Gudlaugsson, S., Richter, B., Friðleifsson, G.Ó., Thorhallsson, S., 2002. Reykjanes high-temperature field, SW-Iceland. Geology and hydrothermal alteration of well RN-10. 27th Stanford Workshop on Geothermal Reservoir Engineering, pp. 233–240.

Friðleifsson, G.Ó., Elders, W.A., Zierenberg, R.A., Fowler, A.P.G., Weisenberger, T.B., Mesfin, K.G., Sigurdsson, Ó., Albertsson, A.L., Níelsson, S., Einarsson, G., Óskarsson, F., Gudnasson, E.Á., Tulinius, H., Hokstad, K., Jóhannesson, Þ., Benoit, G., Nono, F., Loggia, D., Parat, F., Cichy, S.B., Escobedo, D., and Mainprice, D., 2018, The Iceland Deep Drilling Project at Reykjanes: Drilling into the root zone of an analog of a black smoker. Journal of Volcanology and Geothermal Research. 19p. doi.org/10.1016/j.volgeores.2018.08.013.

Friðleifsson, G. Ó., B. Pálsson, B. Stefánsson, A. Albertsson, Þ. Gíslason, E. Gunnlaugsson, J. Ketilsson, S. Sæther, C. Sörlie, W.A. Elders, R.A. Zierenberg, 2020 a, The IDDP Success Story – Highlights. Proceedings World Geothermal Congress.

Friðleifsson G.Ó., A. Albertsson, A. Stefánsson, G. Þórólfsson, K.G. Mesfin, K.V. Matthíasdóttir, K. Sigurðsson, Ó. Sigurðsson, Þ. Gíslason, W.A. Elders, R. A. Zierenberg, E. Bali, E.Á. Guðnason, F. Óskarsson, T.B. Weisenberger, 2020 b, The IDDP-2 DEEPEGS Demonstrator at Reykjanes – Overview. Proceedings World Geothermal Congress.

Gee, M. A. M., M. F. Thirlwall, R. N. Taylor, D. Lowry, and B. J. Murton (1998), Crustal processes: Major controls on Reykjanes Peninsula lava chemistry, SW Iceland, J. Petrol., 39(5), 819–839.

Ghiorso, M. and Evans, B.W., 2008, Thermodynamics of rhombohedral oxide solid solutions and a revision of the Fe-Ti two-oxide geothermometer and oxygen-barometer. American Journal of Science. 308:957-1039.

Henry, D.J., Guidotti, C.V., and Thomson, J.A., 2005, The Ti-saturation surface for low-to-medium pressure metapelitic biotites: Implications for geothermometry and Ti-substitution mechanisms. Amer. Min., 90:316-328.

Hora, J.M., Kronz, A., Möller-McNett, S., and Wömer, G., 2013, An Excel-based tool for evaluating and visualizing geothermobarometry data. Computers &U Geosciences. 56: 178-185.

Huang, R. and Audétat, A., 2012, The titanium-in-quartz (TitaniQ) themobarometer: A critical examination and re-calibration, Geochim. Cosmochim. Acta, 84:75-89.

Kristmannsdóttir, H., 1975. Hydrothermal alteration of basaltic rocks in Icelandic geothermal areas. Proceedings of the 2nd U.N. Symposium on the Development and Use of Geothermal Resources, San Francisco, pp. 441–445.

Lonker, S.W., Franzson, H., Kristmannsdottir, H., 1993. Mineral fluid interactions in the Reykjanes and Svartsengi geothermal systems. Am. J. Sci. 293, 605–670.

Marks, N., Schiffman, P., Zierenberg, R.A., Franzson, H., and Fridleifsson, G.O., 2010, Hydrothermal alteration in the Reykjanes geothermal system: Insights from Iceland deep drilling program well RN-17, Jour. Volcanology and Geothermal Research, 189, 172-190, doi: 10.1016/j.volgeores.2009.10.018.

Putirka, K.D., 2008, Thermometers and barometers for volcanic systems. Minerals, Inclusions, and Volcanic Processes: Reviews in Mineralogy & Geochemistry 69: 61-120.

Reid, M., Vazquez, J.A., and Schmitt, A.K., 2011, Zircon-scale insights into the history of a Supervolcano, Bishop Tuff, Long Valley, Califorina, with implications fo the Ti-in-zircon geothermometer. Contrib. Mineral. Petrol., 161:293-311.

Schiffman, P., R.A. Zierenberg, A.K. Mortensen, G.Ó. Friðleifsson, and W.A. Elders, 2014, High temperature metamorphism in the conductive boundary layer adjacent to a rhyolite intrusion in the Krafla geothermal system, Iceland. Geothermics. 49:42-48, http://dx.doi.org/10.1016/j.geothermics.2012.11.002.

Sun, S. and McDonough, W.F., 1989, Chemical and isotopic systematics of oceanic basalts: implications for mantle composition and processes, in *Magmatism in the Ocean Basins,* edited by A.D. Saunders and M.J. Norry, Geological Soc. Special. Pub., 42: 313-345.

Weisenberger, T. B., Harðarson, B. S., Kästner, F., Gunnarsdóttir, S. H., Tulinius, H., Guðmundsdóttir, V., Einarsson, G. M., Pétursson, F., Vilhjálmsson, S., Stefánsson, H. Ö., and Níelsson S., (2017). Well Report – RN-15/IDDP-2. Drilling in Reykjanes – Phase 4 and 5 from 3,000 to 4,659. ISOR 2017/016, DEEPEGS deliverable 6.4 234p.

Zheng, Y.-F., 1993, Calculation of oxygen isotope fractionation in hydroxl-bearing silicates. Earth Planet. Sci. Lett., 120:247-263.

Zierenberg, R.A., Fowler, A.P.G., Friðleifsson, G.Ó., Elders, W.A., and Weisenberger, T.B., 2017, Preliminary Description of Rocks and Alteration in IDDP-2 Drill Core Samples Recovered from the Reykjanes Geothermal System, Iceland. GRC Transactions, 41: 1599-1615.